

Characterisation of Lean Premixed Laminar Flames in High Pressure using PIV

D. F. Kurtuluş^{*,2}, C. Cohé¹, C. Chauveau¹, I. Gökalp¹

¹Institut de Combustion, Aérothermique, Réactivité et Environnement, CNRS,
1C, avenue de la Recherche Scientifique, 45071 Orléans, Cedex 2, France

²Aerospace Engineering Department, Middle East Technical University,
06531 Ankara, Turkey

Abstract

Laminar flame characteristics of methane-air flames were studied in a Bunsen burner at different pressures and equivalence ratios by using Particle Image Velocimetry (PIV) technique. The experiments are performed in a stainless steel combustion chamber of 300 mm inner diameter and 80 liters volume which could attain a pressure of 1 MPa maximum. A Minilite PIV Nd:YAG laser delivers 25 mJ/pulse at 10 Hz coupled with a spherical lens of 592 mm focal length and a semi-cylindrical lens of 25.5mm. The light scattered by the particles is recorded with a TSI PIV CAM 10-30, at a rate of 10 double images per second, with a time separation between exposures of 150 μ s. PIV technique is used to determine the instantaneous flame front position and flow velocities. The study is performed for pressures of 0.1MPa and 0.2 MPa and equivalence ratios from 0.88 to 1.05. Both conditional and non-conditional measurement methods are employed. Then the results are compared with the CHEMKIN calculations for unstretched flames. The aim of this research was to contribute to the characterisation of CH₄ -air premixed laminar flames at different pressures and equivalence ratios. Indeed, starting from PIV velocity fields and flame contours, the effect of the stretching on the laminar burning velocity is also investigated.

Introduction

The study of laminar flames is the heart of combustion theory. Indeed, the understanding of the laminar premixed flames is a prerequisite for the study of turbulent flames. In the literature, simplified experiments are used to understand the basic properties of combustion as laminar flames, flame/vortex interactions. Laminar burning velocities are fundamentally important for the development and validation of the chemical kinetic mechanisms of the reactive mixture as well as for the prediction of the performances and emissions of several combustion systems [1-2]. The laminar flame speed of a gas mixture depends on various parameters such as the equivalence ratio, pressure and unburned gas temperature.

The effects of flame curvature and stretch on the laminar flame speed have been investigated experimentally and compared to the theoretical predictions by Echekki and Mungal [3]. The flame speed at the tip and side of a slot burner is measured using particle tracking velocimetry, flame tip curvatures are measured using direct flame photography and temperatures are measured using Rayleigh scattering. The flame tip of the Bunsen burner provides a simple geometry of a curved and stretched laminar premixed flame.

The flame speed at the tip S_L defined as the cold gas velocity normal to the flame has been observed to exceed the value of the one-dimensional flame speed, S_L^0 by a significant amount.

An analytical solution for the flame tip based on a constant density approach is given by Sivashinsky [4] and based on variable density by Buckmaster et al. [5-6]. The analytical results of Buckmaster provide implicit solutions of the flame tip curvature as a function of the flame angle at the side.

A set of flame images collected by the CCD camera was analyzed and a map of instantaneous velocity vectors over the cross section of the flame was generated by Ogami and Kobayashi [7]. From this map, the local streamlines were calculated by interpolation. Along each streamline, the point where the magnitude of a velocity vector changes abruptly was determined. The OH-PLIF image was also taken by the ICCD camera at the same time as PTV and the flame front was determined from the OH-PLIF images as the point where LIF intensity begin to increase, and was fitted to the polynomial curve and superposed on the streamlines. By calculating the angle between the tangential line to the flame front and streamline θ , the local burning velocity S_r was obtained at the intersection of the calculated local streamline and the flame front using the equation: $S_r = U_r \sin \theta$ where the laminar flame speed is U_r multiplied with the sine of the angle between the streamlines and the tangent of the flame contour θ (Fig. 1). U_r is the magnitude of the local velocity vector at the front edge of the preheating zone and is taken to be the minimum total velocity along the streamline passing from the contour point.

* Corresponding author: dfunda@ae.metu.edu.tr

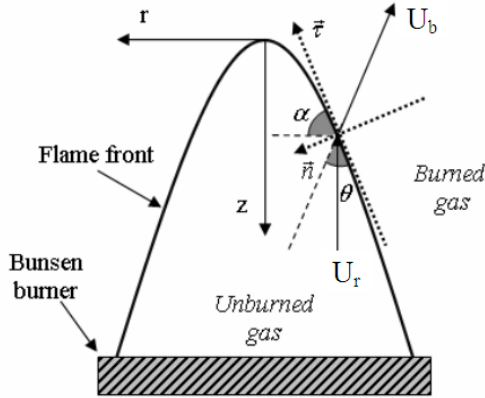


Fig. 1 Flame front parameters.

The paper discusses mainly the pressure effect and equivalence ratio effect on the flame structure.

Experimental setup

The stainless steel cylindrical high pressure combustion chamber of ICARE can sustain premixed flames up to 1 MPa [8-11]. The chamber consists of two cylindrical halves of 600 mm high, each equipped with 4 windows of 100 mm diameter for optical diagnostics (Fig. 2). The internal chamber diameter is 300 mm and the chamber volume is about 80 litres. Water flows through the wall jackets for cooling the chamber. The burners can be placed centrally inside the chamber and can be moved along the chamber vertical z-axis by means of a stepping motor.

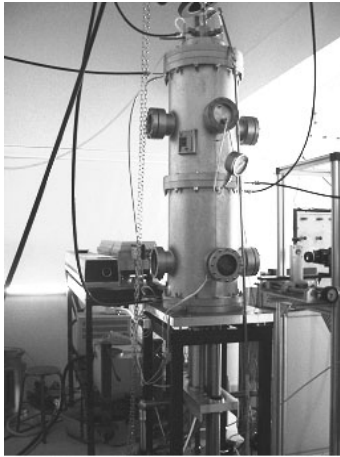


Fig. 2 The high pressure chamber.

The laminar burner (Fig. 3) used in this study generates a conical Bunsen flame configuration and is composed of two blocks. The upper part of the burner has a convergent profile. A porous grid is placed in the bottom part of this section of the burner to obtain a homogeneous laminar flow. The diameter of the burner exit is 12 mm. The lower part is the fixation section to the chamber and to the gas lines [12].

The equivalence ratio varies between 0.7 and 1.05. The outlet velocity U_0 is determined by the competition between the stability of the flame and a low Reynolds

number condition to keep the flame under laminar conditions. If the outlet velocity is too low compared to the laminar flame speed, there is a flashback of the flame in the burner; and if the outlet velocity is too high, a blow off of the flame is observed. The outlet velocity value is in the range of 0.7 - 1 m/s.

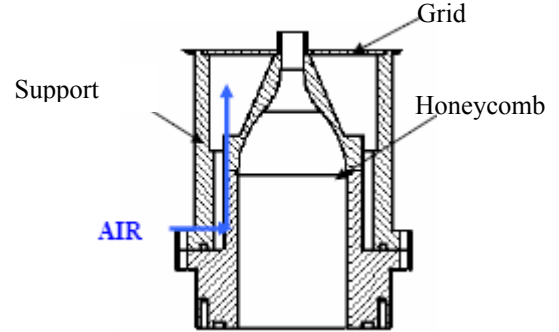


Fig. 3 Laminar burner.

The source of light comes from a Nd-YAG (Continuum Minilite PIV) laser of 532 μm , pulsed to 10 Hz with a power of 25mJ. The laser sheet is generated using a spherical lens of focal distance 592 mm and a semi-cylindrical lens of focal distance 25.5 mm (Fig. 4).

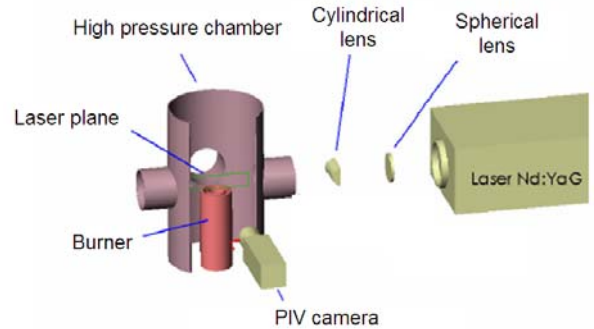


Fig. 4 PIV setup with laminar burner.

Moreover, to avoid any reflection on the burner, the laser sheet crosses a space filter. Camera (TSI PIV-CAM 10-30) and its objective (Nikkor 50 f/1.4D) are placed at 90°. The opening of the camera is of 2,8. One interferential filter centered on 532 μm (+/- 9 nm) is placed in front of the sensor of the camera and allows to eliminate the parasitic lights such as for example the emission from the flame. Finally a system of synchronization (To synchronize laser pulsates TSI) makes it possible to couple the impulses laser and the opening of the camera.

The duration between two images is 150 μs . The resolution of the image (1016x1000 pixel²) is of 32 $\mu\text{m}/\text{pixel}$. Thus the displacement of a particle between two images is of approximately 5 pixels (for a rate of flow of 1 m/s), which is adapted to the study with working areas of 16x16 pixel². Here, we work with windows of 32x32 pixel², which are brought back via the option Adaptive Nyquist Grid to windows of

16x16 pixel². Finally the exposure time of the camera is 66.7 ms.

The choice of seeding is very important in this type of study. Two types of seeding were used, a conditional seeding, by using incense smoke and a non-conditional seeding, by using solid particles. It was necessary to find the best couple smoked/particle, to obtain a double fine seeding, which does not agglomerate and remains homogeneous. Aluminum oxide particles are chosen as solid particles.

Indeed, it was necessary to take account of humidity present in smoke and of the capacity of the solid particles to absorb this humidity. It is proved that smoke starting from fine incense stick (standard "Chinese") is finer and less wet than that of the thick incense sticks (standard "Indian").

Fig. 5 makes it possible to visualize various seeding types separately then combined. Thus with the combination of two seeding, it was possible at the same time to detect the contour of flame and to be a complete velocity field.

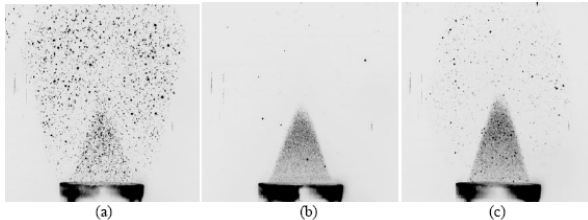


Fig. 5 Different seedings applied for $U_0 = 1$ m/s et $\phi = 0.9$ (a) Solid particle (b) Smoke (c) Solid particle + smoke.

The system set up for the simultaneous use of the two types of seeding is schematized on Fig. 6. Via the various valves, seedings can be used separately or simultaneously. The valves also enable us to control the quantities of the particles or the smoke introduced into the flame.

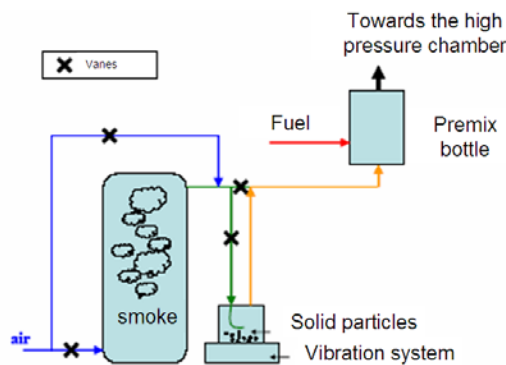


Fig. 6 Seeding system of the experimental setup.

Results and Discussion

The image processing is done in two stages, one consists of obtaining velocity field of the flame using the Insight software of TSI and the other consists of the detection of contour of the flame front starting from a treatment under Matlab. The combination of these two

treatments will make it possible to obtain the flame speed, the stretching and the curvature in each point of the flame front.

A sample instantaneous laminar flame image is represented in Fig. 7 seeded with smoke and aluminum oxide particles. The instantaneous images are filtered by the pixel value corresponding to the minimum pdf of the pixels in the image and binarized accordingly. The binarization procedure distinguishes locally the flame front.

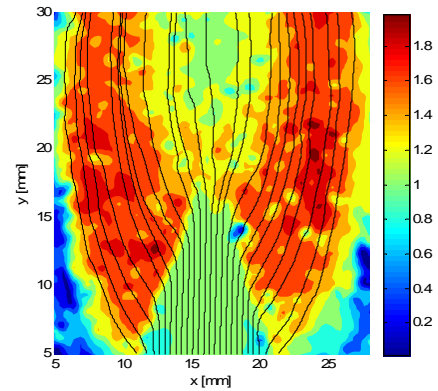


Fig. 7 Instantaneous velocity field.

Moreover, the binarized instantaneous images are averaged by using 300 consecutive images (Fig. 8). The sum of the instantaneous filtered data increases the pixel value inside the unburned gas region due to condensed smoke plus aluminium oxide particles and diminishes the instantaneous influence of aluminium oxide particles in burned gas region.

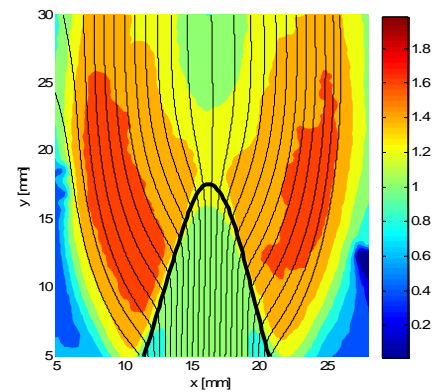


Fig. 8 Average velocity field.

The new averaged image is once more binarized to get the flame contour of the average image (Fig. 9). The pixel corresponding to the minimum pdf value is used for the binarization of the average image. This procedure allows obtaining the flame front contour from the average of the instantaneous images of the field seeded with aluminum oxide and smoke particles. Filtering is used to eliminate the particles at the burned gas region in order to visualize the smoke at the unburned gas region.

With these imaging techniques instantaneous and average flame contours are obtained. Together with the instantaneous and average velocity fields, local flame

propagation velocity and local stretch rates are accurately obtained.

In the following, the variation of the laminar flame velocity data is summarized versus different parameters.

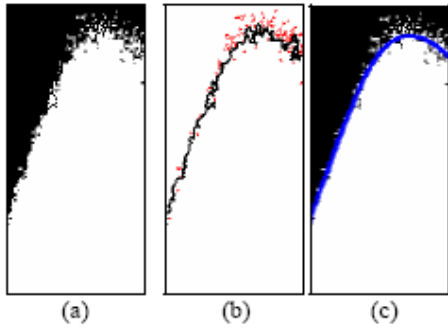


Fig. 9 Contour detection from the binarized image.

The height of flame decreases as the equivalence ratio increases (Fig. 10). The results are given for atmospheric pressure and $U_0=1$ m/s.

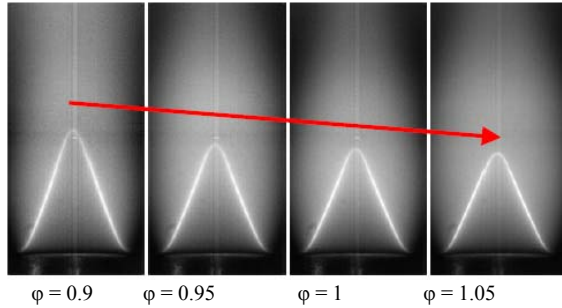


Fig. 10 Laminar flames for different equivalence ratios ($P=0.1$ MPa and $U_0=1$ m/s).

Fig. 11 represents the evolution of the flame front versus pressure. It is observed that the height of flame grows. The height of the cone is approximately 1.5 times the diameter of the burner at atmospheric pressure and 2 times the diameter at 0.2 MPa. Indeed, with the increase in pressure, the laminar burning velocity decreases.

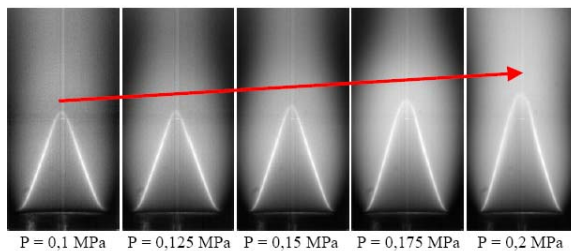


Fig. 11 Laminar flames for different pressures ($\phi = 1$, $U_0=1$ m/s).

With regard to the determination of the laminar burning velocity starting from PIV fields, two methods were tested. The first consists in calculating S_L with the method of the cone:

$$S_L = U_1 \cos \alpha \quad (1)$$

U_1 is the axial speed of fresh gases, and α is the angle between the tangent line of the flame front and the horizontal axis (Fig. 1). U_1 is the mean velocity on the vertical axis in the fresh mixture starting from the burner until the flame front is reached.

The propagation laminar velocity was also calculated with the method of Ogami and Kobayashi [7]:

$$S_L = U_r \sin \theta \quad (2)$$

U_r is local speed at the beginning of the preheating zone. This speed is given by recording the minimal speed on the streamlines of the velocity field. Indeed on a streamline, one observes a decrease of speed and then acceleration due to the thermal expansion of the reaction of combustion (Fig. 12). θ is the angle between the streamline and the tangent to the flame front (Fig. 1).

These two methods are compared for various pressures, at equivalence ratio of 1.05 and $U_0=1$ m/s on Fig. 13. The crosses represent the method of Ogami and Kobayashi [7] and the lines represent the method of the cone. It is noted that these two methods are in very good agreement for different pressures.

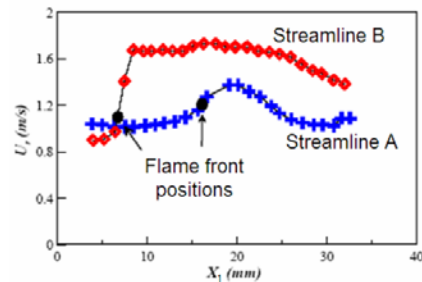
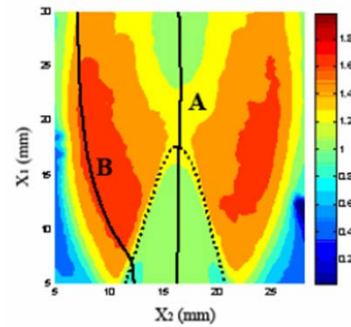


Fig. 12 Evaluation of U_r along two different streamlines of the PIV velocity field.

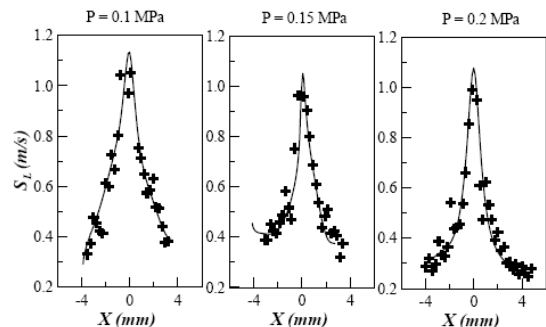


Fig. 13 Comparison of the method of Ogami and Kobayashi [7] (+) and that of the cone (-) for the determination of the laminar burning velocity - $\phi = 1.05$ and $U_0=1$ m/s.

The laminar flame speed obtained by the cone method for no stretch (that is the base region of the flame front where the stretch is zero [11]) is compared on Fig. 14 with the experimental (Ogami and Kobayashi [7]; Hassan et al., [13]; Vagelopoulos et al. [14]) and numerical (Smith et al. [15]) results in the literature.

Two other methods were employed to determine the laminar burning velocity at no stretch. One from the conservation equation, called the surface method. In fact, it is possible to write that $A_{flame}S_L^0 = A_{burner}U_0$, where A_{flame} is the total surface of the flame front and A_{burner} is the area of the burner entrance. The other one is the determination of the laminar burning velocity with the PREMIX code of the Chemkin-II source. The Gri-Mech v.3.0 mechanism is employed.

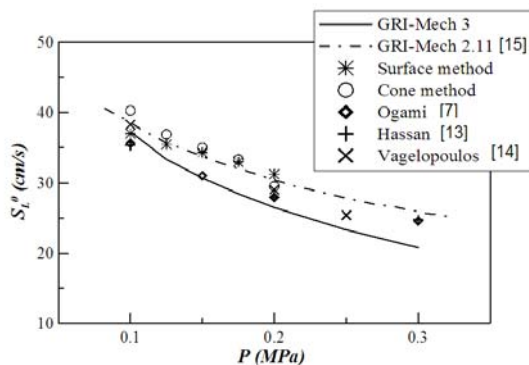


Fig. 14 Laminar burning velocity for no stretch.

The trend is quite good. The experimental results are in good agreement with numerical results using GRI-Mech 2.11 at high pressures. However, the experimental results overestimate the laminar burning velocity when comparing with the GRI-Mech 3 mechanism.

Conclusion

An experimental study on CH₄-air laminar flames at various pressures is conducted by using laminar Bunsen flame configuration. The aim of this research was to contribute to the characterisation of CH₄-air premixed laminar flames at different pressures and equivalence ratios. Indeed, starting from PIV velocity fields and flame contours, it will be possible to study the effect of the stretching on the laminar burning velocity.

Acknowledgments

This work has been supported by the CNRS, the region Centre and the European commission AFTUR project, Alternative Fuels for Industrial Gas Turbines, Contrat ENK5-CT-2002-0062. Dr. Cohé was supported by a joint grant from the CNRS and the Conseil Regional Centre. Dr. Kurtulus acknowledges the support by CNRS- ICARE, TUBITAK and METU.

References

[1] Bradley, D., Hicks, R. A., Lawes, M., Sheppard, C. G. W. and Wolley, R. Measurement of laminar burning velocities and Markstein numbers for iso-octane-n-heptane-air mixtures at elevated temperatures and

pressures in an explosion bomb *Combust. Flame*, 115, pp.126-144, 1998

[2] Liao, S. Y., Jiang, D. M., Huang, Z. H. and Zeng, K. Characterization of laminar premixed methanol-air flames. *Fuel*, 85, pp. 1346-1353, 2006

[3] Echehki, T. and Mungal, M. G. Flame speed measurements at the tip of slot burner: Effects of flame curvature and hydrodynamic stretch. *33rd Symposium (International) on Combustion*, pp. 455-461, 1990

[4] Sivashinsky, G. I. Structure of Bunsen flames. *J. Chem Phys*, 62, pp.638-643, 1975

[5] Buckmaster, J. D. and Crowley, A. B. The fluid mechanics of flame tips. *J. Fluid Mechanics*, 131, pp.341-361, 1983

[6] Buckmaster, J. D. and Ludford, G. S. S. Theory of laminar flames. *Cambridge University Press*, pp.179-185, 1982

[7] Ogami, Y. and Kobayashi, H. (2005) Laminar burning velocity of stoichiometric CH₄/air premixed flames at high-pressure and high-temperature. *JSME International Journal Series B*, 48, 603-609

[8] Lachaux T., Halter F., Chauveau C., Gökalp I., Shepherd I.G., Flame front analysis of high-pressure turbulent lean premixed methane-air flames. *Proc. Combust. Inst.* 30 pp.819-826, 2005.

[9] Cohé C, Chauveau C, Gökalp I, Kurtulus DF, CO₂ addition and pressure effects on laminar and turbulent lean premixed CH₄ air flames, the 32nd International Symposium on Combustion, McGill University, Canada, 3-8 August 2008.

[10] Cohé C, Kurtulus DF, Chauveau C, Gökalp I, Effect of Pressure and CO₂ Dilution on the Flickering of Conical Laminar Premixed Flames, 21st ICDERS, 23-27 July 2007, Poitiers, France

[11] Cohé C, Kurtulus DF, Chauveau C, Gökalp I, Investigation of laminar lean premixed methane-air flames at high pressures, ECM 2007, 3rd European Combustion Meeting, ECM 2007, 11-13 April 2007, Chania, Crete

[12] Cohé C., Caractérisation de l'effet de la pression et de l'ajout de CO₂ sur les flammes laminaires et turbulentes de prémélange pauvre méthane-air, Ph.D thesis, University of Orléans, Orléans, France, 2007.

[13] Hassan, M. I., Aung, K. T. and Faeth, G. M. Measured and predicted properties of laminar premixed methane/air flames at various pressures. *Combust. Flame*, 119, pp. 539-550, 1998

[14] Vagelopoulos, C. M., Egolfopoulos, F. N. and Law, C. K. Further consideration on the determination of laminar flame speeds with counterflow twin-flame technique. *Proceedings of the Combustion Institute*, 25, pp. 1341-1347, 1994

[15] Smith, G. P., Golden, D. M., Frenklach, M., Moriarty, N. W., Eiteneer, B., Goldenberg, M., Bowman, C. T., Hanson, R. K., Song, S., Gardiner, W. C., Lissianski, V. V. and Qin, Z. http://www.me.berkeley.edu/gri_mech/, GRI-Mech Hompage, Gas Research Institute, 1999.